SUPPLEMENTARY INFORMATION:

Design, synthesis and evaluation of fused bicyclo[2.2.2]octene as a potential core scaffold for the non-covalent inhibitors of SARS-COV-2 3CL^{pro} main protease

Barbara Herlah[a,b] Andrej Hoivik[c], Luka Jamšek[c], Katja Valjavec[a], Norio Yamamoto[d], Tyuji Hoshino[e], Krištof Kranjc[c]*, Andrej Perdih[a,b]*

[a]*National Institute of Chemistry, Hajdrihova ulica 19, SI-1000 Ljubljana, Slovenia*

[b]*Faculty of Pharmacy, University of Ljubljana, Aškerčeva 7, SI-1000 Ljubljana, Slovenia*

[c]*Faculty of Chemistry and Chemical Technology, University of Ljubljana, Večna pot 113, SI-1000 Ljubljana, Slovenia*

[d] *Department of Microbiology, Tokai University School of Medicine, 143 Shimokasuya, Isehara, Kanagawa 259-1193, Japan*

[e] *Graduate School of Pharmaceutical Sciences, Chiba University, 1-8-1 Inohana, Chuo-ku, Chiba 260-8675, Japan*

* Corresponding authors:

Krištof Kranjc: **kristof.kranjc@fkkt.uni-lj.si**
Andrej Perdih: **andrej.perdih@ki.si**

1. Molecular interaction fields (MIFs) in the SARS-Cov-2 3CL^{pro} main protease active site

A

B

C
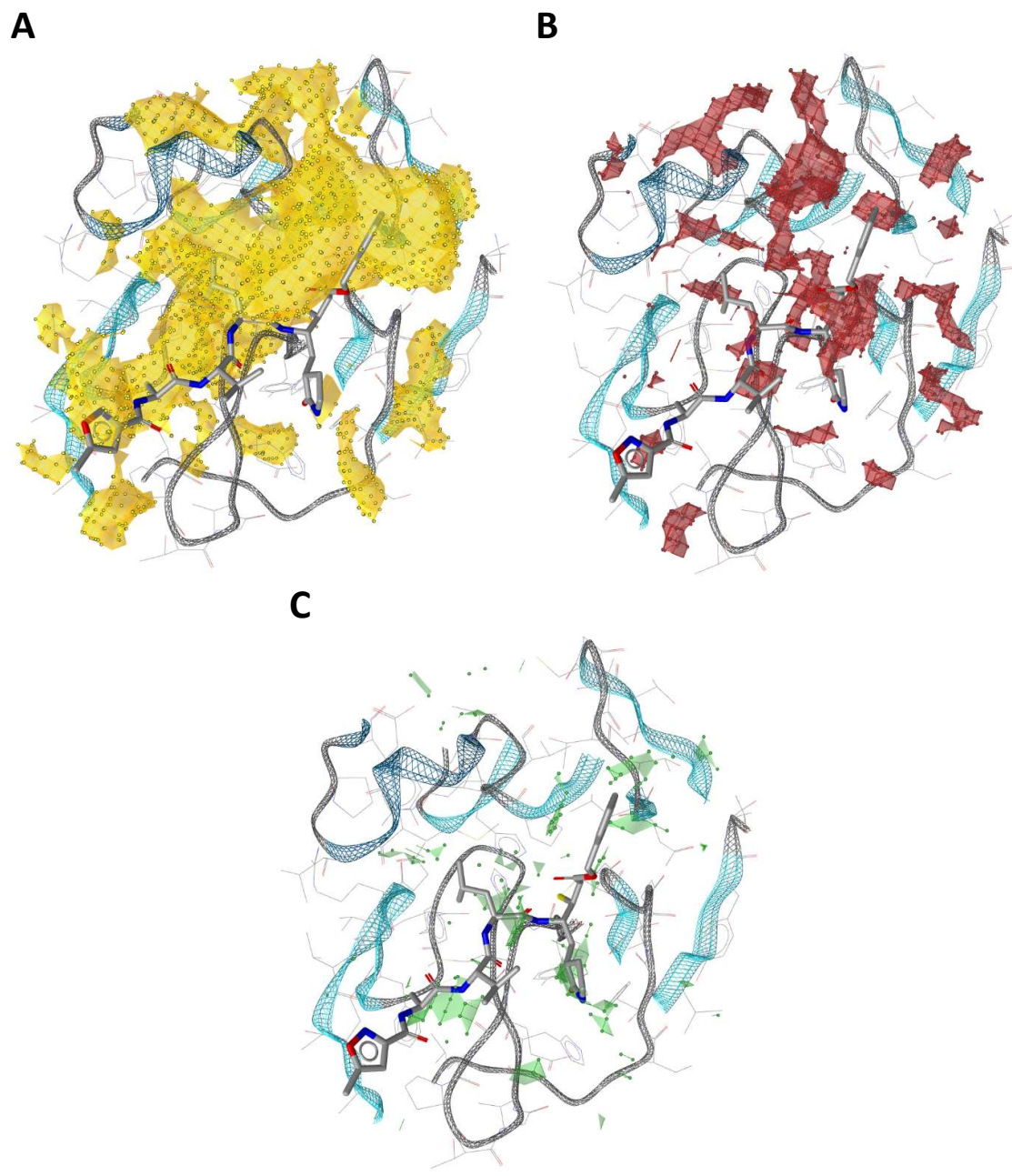
Figure S1. Sars-Cov-2 3CL^{pro} Main Protease. Calculated molecular interaction fields using hydrophobic ((**A**); yellow), hydrogen bond acceptor ((**B**); red) and hydrogen bond donor ((**C**); green) probes, with the bound ligand N3 shown (PBD: 6LU7).

## 2. Molecular docking calculations of HIV-1 protease inhibitors
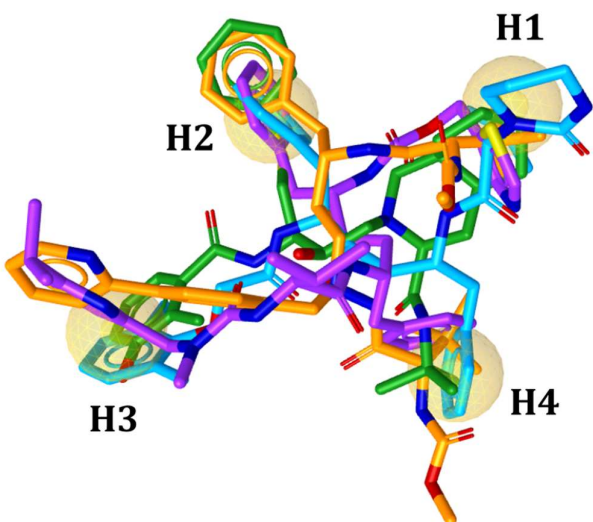
Figure S2. Alignment of docked conformations of HIV-1 protease inhibitors atazanavir (orange), lopinavir (light blue), nelfinavir (green) and ritonavir (violet). The compounds contain four hydrophobic moieties that can fit into four sub-pockets of the 3CL^{pro} active site (PDB: 6LU7).

## 3. Ligand docking position and ligand movement during molecular simulation
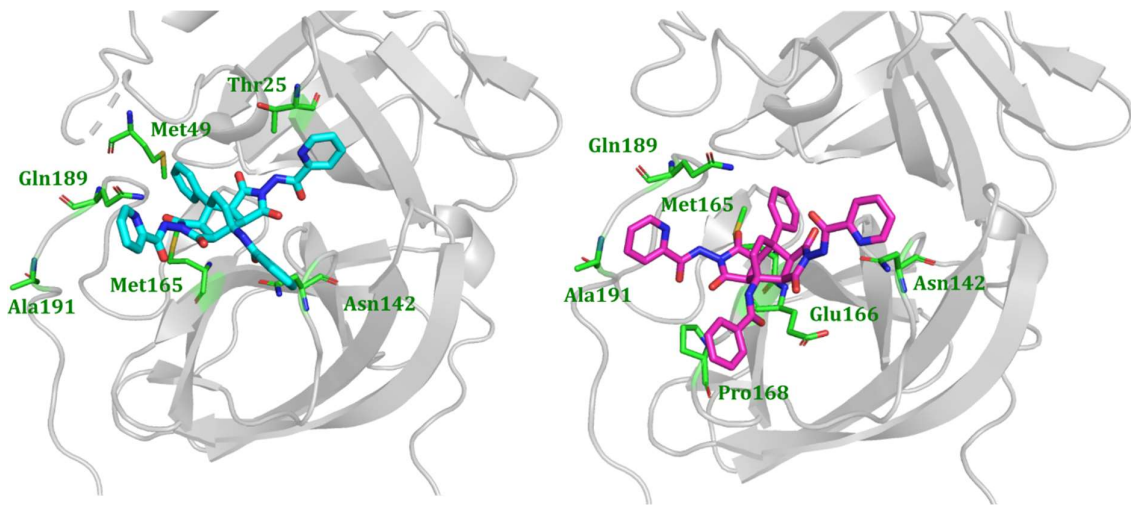
Figure S3. Ligand shift during the molecular dynamics simulation (left) Ligand **11a** in its initial docked position located between domains I and II of 3CL^{pro}, (right) Shifted position of **11a** towards the 3CL^{pro} domain II after the 120 ns MD mark. (PDB: 6LU7) .

## 4. Comparison with x-ray covalent inhibitor
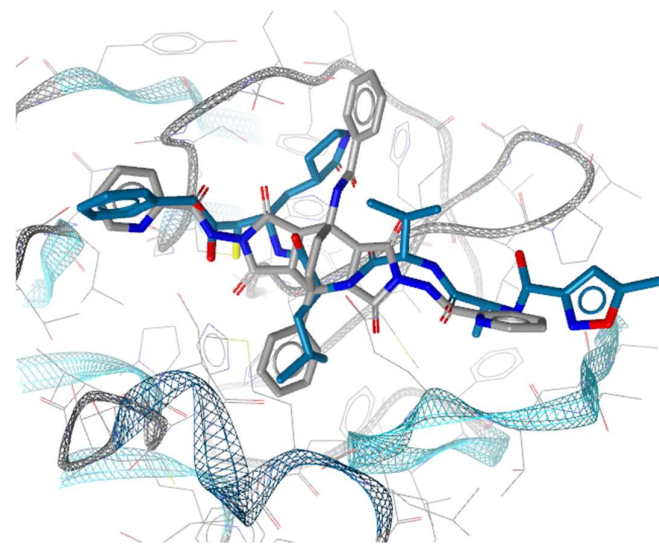
Figure S4. Comparison of the experimental conformation of covalent inhibitor bound in the 3CL[pro] X-ray structure and docked position of the ligand **11a** (PDB: 6LU7) .

5. Analysis of molecular dynamics simulation
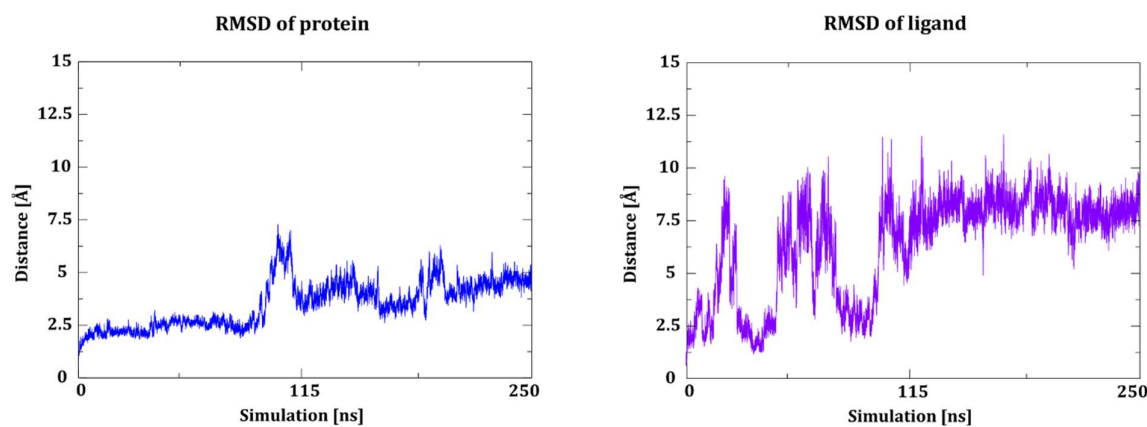
Figure S5. (left) Time-dependent RMSD of the 3CL[pro] protein (Cα atoms) (right), Time-dependent RMSD of the ligand **11a**.

6. Screening of SARS-CoV-2 3CL^{pro} main protease inhibition
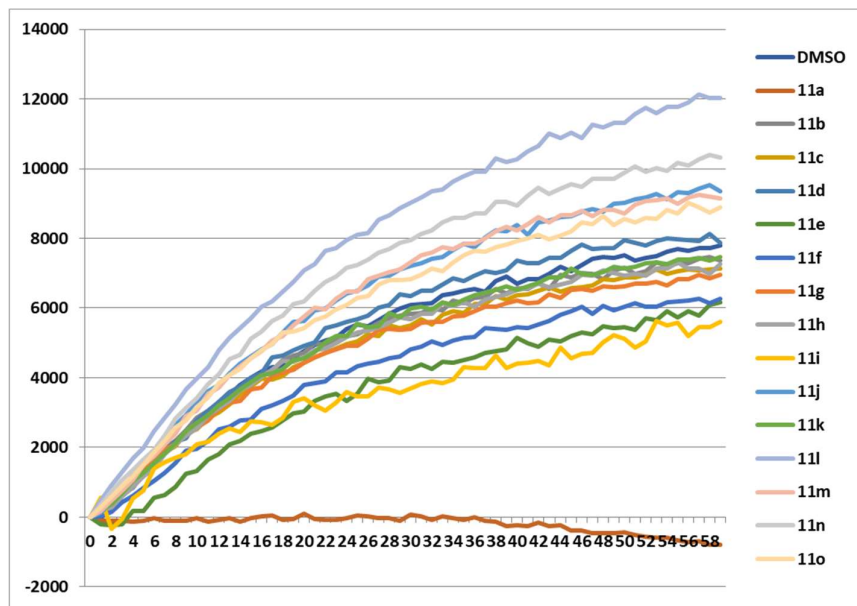
Figure S6. Experiments with 3CL^{pro} protease **3CL(+)** fluorescence intensity on y-axis is calculated from the value of F(t) – F(0). 64 µM concentration of bicyclo[2.2.2]octenes **11a–o** is used and x-axis is time in minutes.
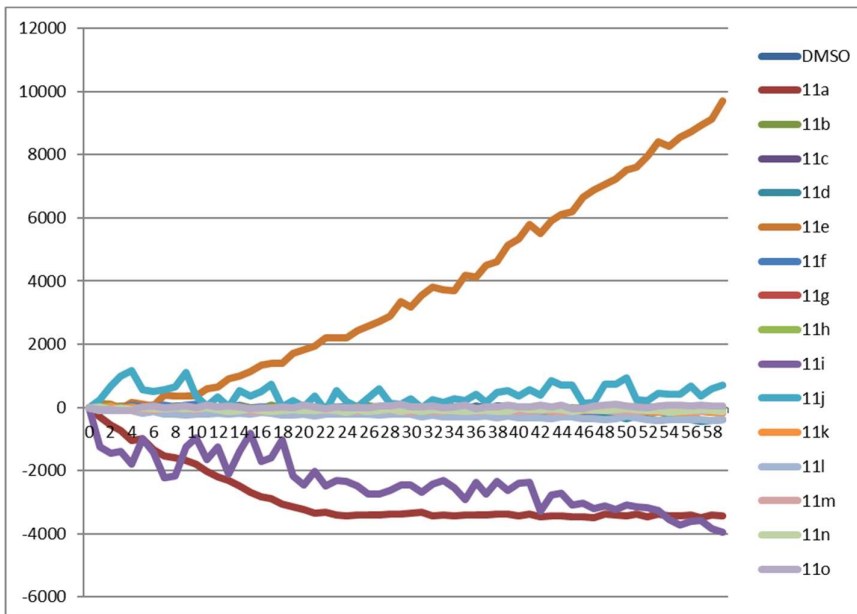
Figure S7. Experiments without 3CL^{pro} protease **3CL(-)** Background fluorescence intensity (y-axis) 64 µM concentration of bicyclo[2.2.2]octenes **11a–o** is used and x-axis is time in minutes.
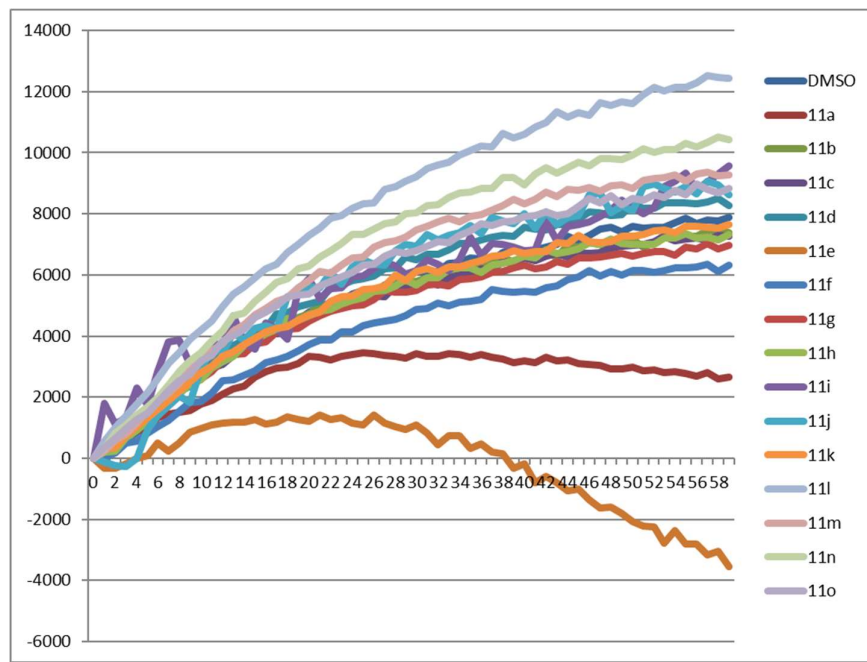
Figure S8. Data showing the difference between **3CL(+)** and **3CL(-)** 64 μM concentration of bicyclo[2.2.2]octenes **11a–o** is used and x-axis is time in minutes.

7. Partial charges and atom types of the simulated compound 11a

Table S1: Atom types and partial atomic charges for compound **11x** from the General Amber Force Field (gaff).
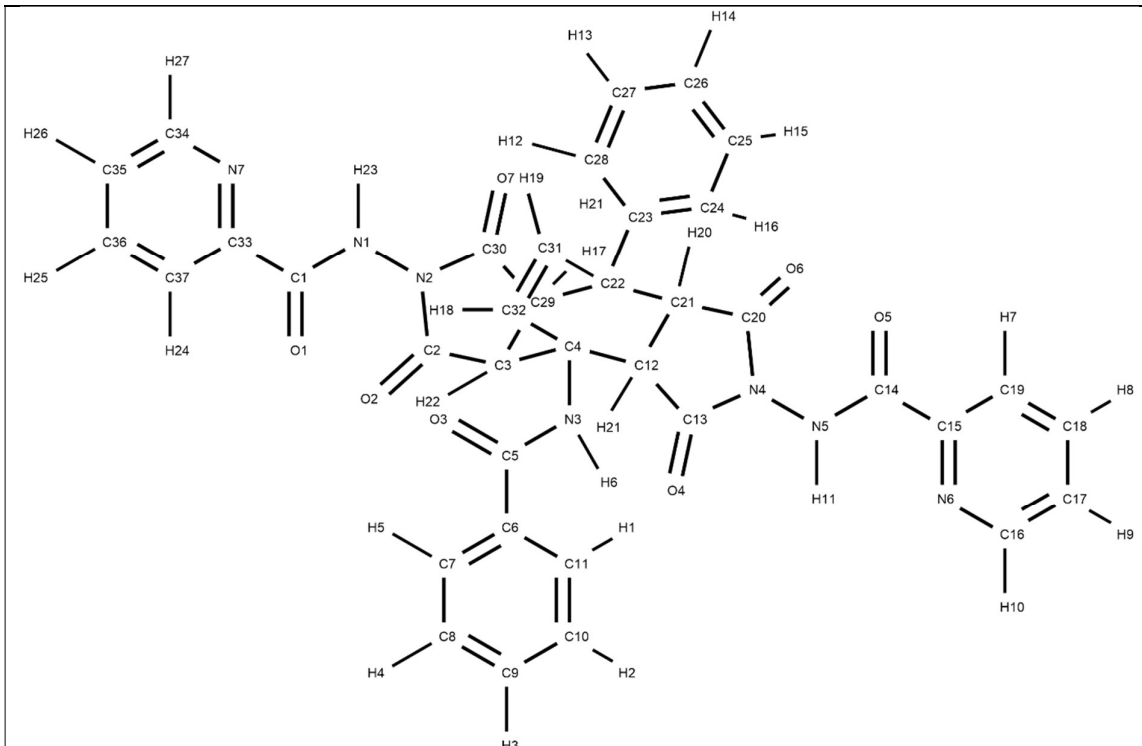
| Name	Type	q	Name	Type	q	Name	Type	q
C10	ca	-0,15539	**C1**	c	0,650584	**H14**	ha	0,12667
C11	ca	-0,09455	**O1**	o	-0,56292	**H15**	ha	0,131839
H1	ha	0,141117	**C33**	ca	0,395204	**H16**	ha	0,148091
H2	ha	0,136021	**N7**	nb	-0,59114	**C21**	c3	-0,34489
C9	ca	-0,08345	**C34**	ca	0,35777	**C20**	c	0,695319
H3	ha	0,126235	**C35**	ca	-0,38728	**O6**	o	-0,52909
C8	ca	-0,15539	**C36**	ca	0,134943	**H20**	hc	0,077115
H4	ha	0,136021	**C37**	ca	-0,36656	**C12**	c3	-0,05793
C7	ca	-0,09455	**H24**	ha	0,176752	**H21**	hc	0,122113
H5	ha	0,141117	**H25**	ha	0,10953	**C13**	c	0,550358

C6	ca	-0,1197	**H26**	ha	0,173901	**O4**	o	-0,50033
C5	c	0,82655	**H27**	h4	0,056608	**N4**	n	-0,08768
O3	o	-0,60723	**H23**	hn	0,340706	**N5**	n	-0,56424
N3	n	-0,8271	**C30**	c	0,695319	**H11**	hn	0,340706
H6	hn	0,324279	**O7**	o	-0,52909	**C14**	c	0,650584
C4	c3	0,454682	**C29**	c3	-0,34489	**O5**	o	-0,56292
C32	c2	-0,28834	**H17**	hc	0,077115	**C15**	ca	0,395204
C31	c2	-0,30281	**C22**	c3	0,38365	**N6**	nb	-0,59114
H19	ha	0,160165	**C23**	ca	0,013663	**C16**	ca	0,35777
H18	ha	0,219125	**C24**	ca	-0,17875	**H10**	h4	0,056608
C3	c3	-0,05793	**C25**	ca	-0,1207	**C17**	ca	-0,38728
H22	hc	0,122113	**C26**	ca	-0,11945	**H9**	ha	0,173901
C2	c	0,550358	**C27**	ca	-0,1207	**C18**	ca	0,134943
O2	o	-0,50033	**C28**	ca	-0,17875	**H8**	ha	0,10953
N2	n	-0,08768	**H12**	ha	0,148091	**C19**	ca	-0,36656
N1	n	-0,56424	**H13**	ha	0,131839	**H7**	ha	0,176752

8. Selected examples of 1H and 13C NMR spectra: compounds 11a and 11e

11e

11.404
11.125
8.973
8.777
8.768
8.173
7.875
7.859
7.724
7.597
7.537
7.521
7.445
7.309
7.293
6.717
6.600
4.810
4.795
4.754
4.739
4.182
4.167
4.058
3.332
2.502
2.406

0.000

0.87
0.99
2.00
1.95
2.01
3.14
6.06
2.03
2.02
0.96
2.03
2.03
3.07

10.0   5.0   0.0

ppm (f1)

11e

171.401
170.998
168.575
163.092
153.214
153.094
148.557
138.812
138.368
138.059
135.472
131.457
128.266
127.773
127.443
126.927
126.665
126.574
123.804

59.824
47.458
45.692
42.278
39.500
19.006

200   150   100   50   0

ppm (f1)

10